Indian Journal of Chemistry
Vol. 64, February 2025, pp. 213-224
DOI: 10.56042/ijc.v64i2.15602

Synthesis and characterization of (E)-N-carbamimidoyl -4 and (E)-4- benzenesulfonamides; biological study, DFT, molecular docking, and ADMET predictions

Adeleke A Adenıyı*[a], Abdullahı O Sobola[a,b], Mutıu O Sowemımo[a], Gbolahan S Towolawı[c] & Rıdwan Sulaımon[d]

[a] Department of Chemistry, Lagos State University, Lagos-Badagry Expressway, Ojo, 102101, Lagos, Nigeria

[b] Afrıcan Centre of Excellence for Innovative and Transformative STEM Education (ACEITSE), Lagos State University, Ojo, Lagos, Nigeria

[c] Department of Chemistry & Nanoscale Science, University of North Carolina, Charlotte, North Carolina, USA

[d] Department of Chemistry and Biochemistry, Concordia University, Montreal, Quebec, Canada

Email: adeleke.adeniyi@lasu.edu.ng

Received 09 December 2024; accepted(revised) 22 January 2025

Sulphonamide Schiff bases (L_1 and L_2) containing imidazole nuclei have been synthesized and evaluated for their antimicrobial and antioxidant activity. Sulfaguanidine and sulfamerazine have been condensed with 4-methyl-5-imidazolecarboxalehyde to obtain ligands L_1 and L_2, respectively. The compounds have been characterized by FT-IR, ^{1}H and ^{13}C NMR, UV-Vis, CHNS, and MALDI-TOF mass spectral data. The antimicrobial activity of the sulphonamide-derived Schiff bases have been conducted using agar well diffusion against *S. aureus*, *B. substilis*, *E. Coli*, *Salmonella spp*., and *Candida spp*. Similarly, the free radicals scavenging activity of the compounds has been evaluated at 20 – 100 µg/mL using DPPH (1,1'-diphenyl-2-picryl-hydrazil), nitric oxide, and hydrogen peroxide antioxidant assays. Both compounds exhibited moderate activity against *Salmonella spp*. However, L_1 exhibits higher radical scavenging ability than L_2 against NO free radicals at low to high concentrations with IC_{50} values of 84.50 and 101.59 µg/mL for L_1 and L_2, respectively. Ligand L_2 is however, more active than L_1 against H_2O_2 free radicals at low concentrations (20 – 60 µg/mL). The optimized geometries of the compounds have been docked at the active sites of cytochrome oxidase, myeloperoxidase, NADPH oxidase, xanthine oxidase, dihydropteroate synthase (DHPS), and dihydrofolate reductase (DHFR) proteins.

Keywords: *In silico*, Schiff bases, DPPH assay, Imidazole, Antioxidants, Antimicrobial

The World Health Organization (WHO) has declared antimicrobial resistance (AMR), a threat to global health and development. The emergence of drug-resistant microbial strains threatens the effectiveness of most clinically available therapeutic agents, especially sulfa drugs. Consequently, there is a dire need to continuously design novel therapeutic agents with enhanced potency. The first clinically synthetic anti-microbial drug was prontosil, a sulphonamide-based anti-bacterial agent[1]. Most sulphonamide-based drugs are sulphanilamide derivatives, and each sulfa drug is characterized by a specific substituent, R, at the amido nitrogen of the sulphanilamide moiety. Structurally, sulphonamides are aniline-derived organosulphur compounds containing the $–SO_2NH_2$ or SO_2NH- moiety. The substituent variation has given rise to a series of sulphonamide drugs with varying pharmacological activity and toxicity. For instance, silver sulfadiazine treats and prevents bacterial infection in people with severe burns, while sulfapyridine and sulfamethoxazole are effective against dermatitis herpetiform and urinary tract infections, respectively.

Sulphonamides prevent bacterial growth and multiplication by inhibiting the bacterial enzyme dihydropteroate synthase (DHPS) in the folic acid pathway, thereby preventing bacterial nucleic acid synthesis[2]. Sulphonamide-based drug agents have a broad spectrum of pharmacological activity as anti-bacterial[3], anti-viral[4], anti-inflammatory[5], anti-tumour[6], antioxidants and[7], anti-fungal[8], among others. Sulfa drugs have equally been administered for the treatment of other various non-microbial conditions as protease inhibitors in HIV antivirals[9], carbonic anhydrase inhibitors in the treatment of glaucoma[10], loop diuretics for heart failure management and[11], coX-2 inhibitors as anti-inflammatory agents[12].

However, resistance to sulphonamide-based drugs is common, and a host of spontaneous mutants of the DHPS enzyme have been isolated from several resistant bacterial strains[13]. The resistance mechanism to sulphonamide drugs has been established to involve the genetic mutation of the dihydropteroate synthase enzyme, thereby lowering the affinity of sulphonamides for the inhibiting enzyme[14]. There have been reported cases of resistance to the trimethoprim-sulphonamide combination. Resistance to trimethyl prim-sulfadiazine has been attributed to point mutations in DHFR and DHPS, which reduce their affinity for pyrimethamine and sulfadiazine, respectively[14].

Schiff base compounds have diverse pharmacological effects as antimicrobial, anti-fungal, anti-inflammatory, anti-viral, anti-tumour, and antioxidant activity[15–17]. The biological activity of Schiff base compounds has been linked to the presence of the amine functional group. Introducing other functional groups, such as the azomethine, C=N, into the sulphonamide scaffolds could lead to a new set of sulphonamide conjugates with enhanced potency and less cellular toxicity. The aim of this study, therefore, is to modify the structures of some clinically available sulphonamide drugs through the formation of Schiff base scaffolds by condensing two sulphonamide drug agents with heterocyclic carboxaldehyde containing the imidazole nucleus, respectively. This is to ascertain their potential robustness in tackling some of the existing AMR challenges.

Experimental Section

The analytical grade chemicals and reagents used for the synthesis were procured from Sigma-Aldrich and used without further purification. The Fourier-transform infrared and the electronic spectral data of the compounds were recorded on Agilent Cary 630AT FT-IR and Shimadzu UV-1900 spectrophotometer, respectively. At the same time, the elemental analysis, CHNS, was done on Varıo El cube CHNS analyzer. The ^{1}H- and ^{13}C-NMR analysis was done in deuterated dimethylsulfoxide (d_6) using a Bruker NMR spectrometer operating at 300 MHz. In addition, their respective mass spectra were recorded on the MALDI-7090 time of flight mass spectrometer. The melting points of the compounds were determined using the Stuart SMP30 melting point apparatus. The compounds were screened against four bacterial (*viz*: *S. aureus, B. substilis, E. Coli, and Salmonella spp.*) and one fungal (*Candida spp.*) strain using the agar well diffusion technique. Similarly, the radical scavenging ability of the Schiff base compounds was evaluated using DPPH (1,1'-diphenyl-2-picryl-hydrazil), nitric oxide, and hydrogen peroxide antioxidant assays. The theoretical calculations for the geometry optimizations and electronic properties were performed using the Gaussian 16 software package using density functional theory (DFT) with B3LYP/6-31G* functional and basis set. A docking study was conducted with AutoDock Vina, utilizing protein and ligand data and grid box properties specified within the configuration file.

Synthesis of the sulphonamide Schiff bases

The sulphonamide Schiff bases were prepared by condensing an equimolar amount of 4-methyl-5-imidazole carboxaldehyde with sulfaguanidine and sulfamerazine under reflux conditions for 6 h, as illustrated in Scheme 1[18].

L_1: (E)-N-carbamimidoyl-4-(((4-methyl-1*H*-imidazol-5-yl)methylene)amino)benzenesulfonamide

A solution of 13.62 mmol (2.91 g) of sulfaguanidine in 10 mL hot dimethylformamide (DMF) was added to a solution of 13.62 mmol (1.50

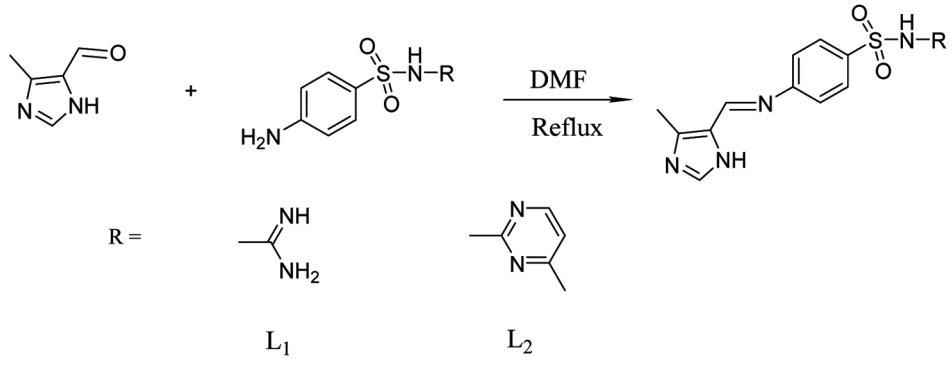

Scheme 1 — Synthesis of the sulphonamide Schiff bases. 3-methyl- imidazole carboxaldehyde was condensed with sulfaguanidine (L_1) and sulfamerizine (L_2).

g) 4-methyl-5-imidazole carboxaldehyde in the same solvent. The mixture was heated under reflux for 6 h to obtain a cream solution. The resulting solution was allowed to cool at room temperature, and a cream precipitate was obtained after three days. The precipitate was filtered under suction, washed with DMF, and recrystallized from the DMF/methanol solvent mixture. Yield: 40.24% (1.676 g).

L_2: (E)-4-(((4-methyl-1*H*-imidazol-5-yl)methylene) amino)- N-(4-methylpyrimidin-2-yl)benzenesulfonamide

13.62 mmol (3.59 g) of sulfamerazine was refluxed with 13.62 mmol (1.50 g) of 4-methyl-5-imidazolecarboxalehyde in DMF for 6 h to obtain a brown solution. The solution was kept at room temperature for three weeks to obtain a dark brown precipitate. The precipitate was filtered under suction, washed with DMF, and dried in a desiccator. Yield: 61.89% (3.00 g).

Antimicrobial study

The synthesized ligands were screened for their bacterial and fungal growth inhibitory activity against *S. aureus*, *B. substilis*, *E. coli*, *Salmonella spp*., and Candida spp. using the agar-well diffusion method[19]. Gentamicin and procolazol were used as the antibacterial and antifungal control agents, while the test compounds were screened at a 10 ppm concentration.

Antimicrobial susceptibility screening

An overnight broth culture of each bacterial isolate corresponding to 3.0×10^7 cfu/mL (MF standard) was inoculated unto sterile Mueller Hinton agar plates. The seeded plates were rocked for an even distribution of isolates, and 10 mm diameter holes were bored on the plates after they were set using a standard cork borer. 10 ppm of the compound was transferred into the well using a micropipette. The plates were kept at room temperature for 1 h to ensure proper diffusion of the compounds before incubating them at 37°C for 24 h. The assay was carried out in triplicate, and the zone of inhibition was measured and recorded in millimetres. The procedure was repeated for the anti-fungal susceptibility test against *Candida spp.* using potato dextrose agar (PDA).

MIC and MBC assays

The minimum inhibitory concentration (MIC) assay was carried out using the agar diffusion method to establish the susceptibility of *Salmonella spp*. against the sulphonamide Schiff base compounds[20]. A diluted concentration series of 10, 5, 2.5, 1.25, and 0.625 ppm of the compounds were prepared using serial dilution and placed aseptically into each labeled section on the plate using a sterilized pipette. The wells were then inoculated with 0.1 mL of the bacterial suspension and incubated at 37°C for 24 h. The wells were observed for growth and death of the test organism, and the lowest concentration that completely inhibited the visual microbial growth was taken as the MIC.

The minimum bactericidal concentration (MBC) is the lowest concentration of the test compounds that prevent the growth of the bacterial strain. The MBC for the compounds was determined using organisms that were uniformly streaked on labeled quadrants using a wire loop. The microorganisms were incubated at 37°C for 24 h, after which growth was observed and recorded. The quadrant with the lowest concentration of the test compounds corresponds to the MBC.

Antioxidant Study

The synthesized sulphonamide-derived Schiff bases compounds, ligands L_1 and L_2, were evaluated for their ability to scavenge free radicals against DPPH, hydrogen peroxide, and nitric oxide free radicals. Ascorbic acid, vitamin C, was used as the reference antioxidant drug, while the antioxidant bioassays were carried out at a concentration range of 20 – 100 μg/mL.

DPPH bioassay

1 mL of 0.1 M DPPH solution was added to various concentrations (20 – 100 μg/mL) of the sulphonamide Schiff bases and the reference antioxidant drug as described in the Blois method[21]. The reduction in the DPPH free radical in the resulting mixtures was measured as absorbance at 517 nm after 30 min. The assay was done in triplicate, and the percentage radical scavenging activity of the compounds is computed as indicated in equation 1:

$$\% \text{ scavenging activity} = \frac{(\text{Absorbance control} - \text{Absorbance sample})}{\text{Absorbance control}} \times 100 \quad ----(1)$$

Similarly, the nitric oxide assay was conducted using sodium nitroprusside and Griess reagents[22], while the Ruch method was employed for the hydrogen peroxide scavenging activity[23].

In silico study

The synthesized ligands were further studied *in silico* to predict their molecular interactions with various target proteins using theoretical calculations and docking studies. Similarly, the drug-likeness, cellular bioavailability, and toxicity of the compounds were also considered.

DFT study

The structures of the two sulphonamides Schiff bases, L_1 and L_2, were subjected to theoretical modeling using density functional theory (DFT) with B3LYP functional and 6-31G* basis set to obtain their optimized geometries[18]. The vibrational frequencies and the electronic properties of the compounds were calculated for the optimized geometries using the same theory. The electronic molecular descriptors calculated for the optimized geometries include the highest occupied molecular orbital (HOMO), lowest unoccupied molecular orbital (LUMO), electronic transition energy gap (ΔE), global hardness (η), ionization energy (I), and electrophilicity (ω).

Docking study

To elucidate the molecular basis of the observed antimicrobial and antioxidant activities exhibited by the ligands under investigation, molecular docking studies using AutoDock Vina were performed[24]. X-ray crystallographic structures of target proteins, including cytochrome peroxidase, myeloperoxidase, NADPH oxidase, xanthine oxidase, dihydropteroate synthase (DHPS), and dihydrofolate reductase (DHFR), were retrieved from the Protein Data Bank (https: www.rcsb.org/), with PDB IDs 4AAO[25], 6WY7[26], 7U8G[27], 1N5X[28], 5V7A[29]and 8E4F[30] respectively. Each protein structure was preprocessed using the BIOVIA Discovery Studio 2021 Visualizer (https://discover.3ds.com/discovery-studio-visualizer-download), and binding pockets were identified with FPocket Web 1.0.1[31].

Optimized structures of the compounds L_1 and L_2 were used for docking. Preparation of pdbqt files for proteins and ligands, including grid box specification, with AutoDock Tools (ADT). ADT was used to assign polar hydrogens, united atom Kollman charges, solvation parameters, and fragmental volumes to the proteins. The prepared files were then saved in pdbqt format. AutoGrid was utilized to generate grid maps by defining a grid box centered on the previously identified binding pockets. Scoring grids based on the ligand structures were created to enhance computational efficiency.

Docking was conducted with AutoDock Vina, utilizing protein and ligand data and grid box properties specified within the configuration file. AutoDock Vina employs an iterated local search global optimizer[24]. For each docking procedure, the conformation with the lowest binding energy and minimal root-mean-square deviation (RMSD) was selected and aligned with the receptor structure for further analysis.

ADMET properties and drug-likeness

The absorption, distribution, metabolism, excretion, and toxicity (ADMET) properties of L_1 and L_2 were thoroughly assessed using the bioinformatics web server ADMETlab3.0 (https://admetlab3.scbdd.com/server/evaluationCal)[32]. This tool was chosen for its comprehensive ADMET prediction capabilities, including analysis of drug-likeness, permeability, bioavailability, and toxicity. Moreover, molecular properties such as molecular weight (MW), hydrogen bond donors and acceptors, and the partition coefficient (LogP) were also calculated to preliminarily assess its potential as an orally active drug candidate based on Lipinski's rule of five[33].

Results and Discussion

The analytical and spectral data for the sulphonamide Schiff bases are presented in Table 1. The mass spectra of both L_1 and L_2 exhibit a prominent peak at 307.749 and 357.258, respectively, corresponding to the $[M+H]^+$ion. The proposed fragmentation patterns for L_1 and L_2 are presented in Schemes 2 and 3, respectively. The molecular weight (calculated) for L_1 and L_2 are 306.349 and

Table 1 — Analytical data of the sulphonamide Schiff bases

Compd	M.F	Mwt g/mol	%Yield	MP°C	[a]Found (Calculated)				[a]$(M+H)^+$ m/z
					%C	%H	%N	%S	
L_1	$C_{12}H_{14}N_6O_2S$	306.09	40.24	228-230	44.63 (44.58)	5.89 (5.44)	28.05 (28.30)	10.89 (10.82)	307.49
L_2	$C_{11}H_{16}N_6O_2S$	356.11	61.89	269-270	44.63 (44.58)	5.89 (5.44)	28.05 (28.30)	10.89 (10.82)	357.28

[a]The analytical data were obtained from the CHNS and MALDI-ToF mass spectrometry analyses

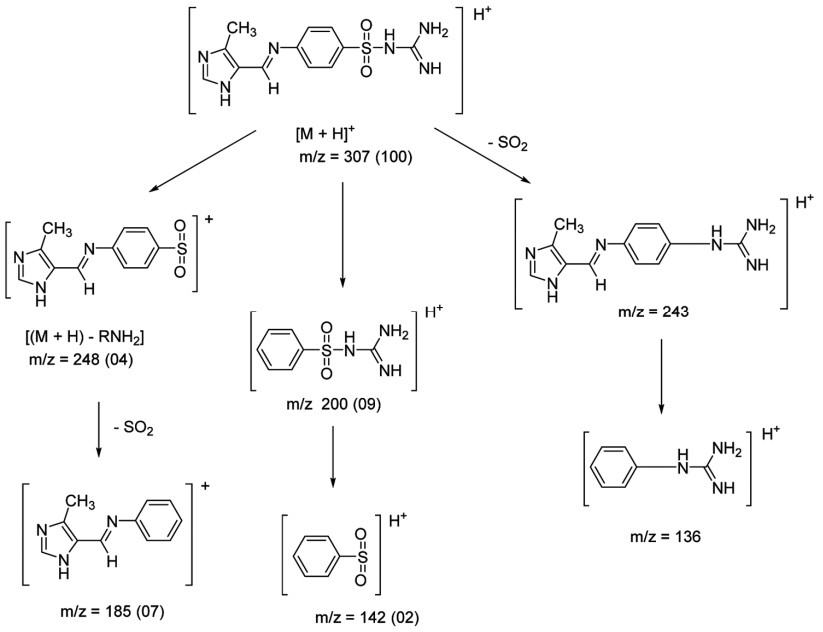

Scheme 2 — Proposed fragmentation pattern for L_1 showing the likely fragment ions obtained from the MALDI-ToF mass spectrometry analysis

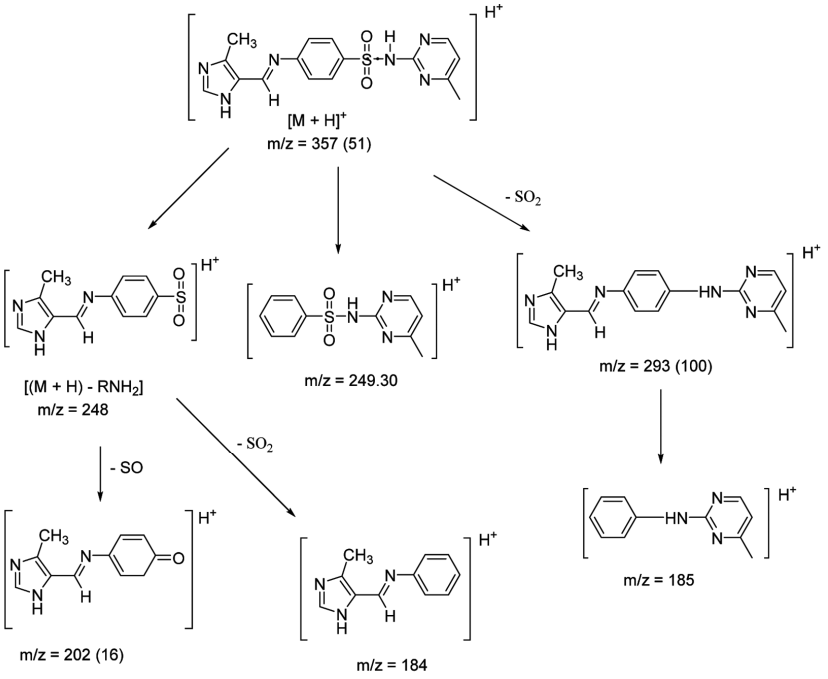

Scheme 3 — Proposed fragmentation pattern for L_2 showing the likely fragment ions obtained from the MALDI-ToF mass spectrometry analysis

356.409g/mol, respectively. In addition, the $[(M+H)-SO_2]^+$ peak was visible in the spectrum of compound L_2, corresponding to the loss of SO_2 gas. The mass spectra for the two compounds are presented as supplementary data S_1 and S_2.

Spectral data

The spectral data for the compounds are presented in Table 2, while the various spectra are presented as supplementary data/Figs. S_3 – S_9. The FT-IR spectrum of ligand L_1 exhibits bands at 3425 cm^{-1} and 3317 cm^{-1}

Table 2 — [a]Spectral data for the sulphonamide Schiff bases

Compd	ν N-H (cm^{-1})	νC=N (cm^{-1})	ν C=C (cm^{-1})	δ O=S=O (cm^{-1})	λ (nm)	1 H-NMR (ppm)	13C-NMR (ppm)
L_1	3425, 3317, 3232	1657 (sulfa) 1629 (imine) 1606 (Imidz)	1580	1342 (asym) 1185 (sym)	272, 322	8.47(1H, s, CH=N), 7.75–7.73(4H, d), 9.78(1H, s, -CH), 7.26(2H, s, br, NH_2), 6.71(3H, s, br, -NH), 2.44(3H, s, $-CH_3$)	158.61(C=N, imine), 158.29 (C=N, sulfa), 155.17(C=N, Imidazole), 151.92(C=C, Imidazole), 141.36, 137.90, 131.30, 127.79, 127.35, 121.40, 112.85(C=C, Ar), 12.36($-CH_3$)
L_2	3481, 3380	1565 (sulfa) 1628 (imine) 1595 (Imidz)	1490	1323 (asym) 1189 (sym)	354	8.31(1H, s, CH=N), 7.76-7.68(4H, d), 6.88(1H, s, -CH), 6.57-6.54(2H, d), 5.99(2H, br, -NH), 2.36 (3H, s), 2.30(3H, s, $-CH_3$)	168.51(C=N, imine), 158.17, 157.45(C=N, sulfa), 153.50(C=N, imidazole), 130.60, 130.21, 125.44, 115.30, 112.52, 90.29 (Ar-C), 23.89($-CH_3$)

[a]The spectral data were obtained from the IR, UV, 1H-NMR, and 13C-NMR analyses.

due to the sulfa ($-SO_2NH$) and the imidazole N-H stretch, respectively, while the third band at 3232 cm^{-1} corresponds to the free NH_2 of the sulfa moiety[18]. Similarly, the N-H stretch for ligand L_2 was observed at 3481 cm^{-1} and 3380 cm^{-1}. However, the N-H bending band for the two ligands was observed at 1565 – 1543 cm^{-1}. Furthermore, the azomethine, C=N, vibration band for the sulphonamide Schiff base ligands appeared at 1629-1628 cm^{-1}[32]. In addition, the strong band at 1657 cm^{-1} in the spectrum of ligand L_1 corresponds to the terminal C=NH group of the sulfa moiety. The formation of the Schiff base compounds was further substantiated by the absence of the aldehyde band at 1680 – 1670 cm^{-1}[34]. The asymmetric SO_2 band of the sulfa moiety was observed at 1343 cm^{-1} and 1323 cm^{-1} for L_1 and L_2, respectively, while the symmetric band appeared at 1185 cm^{-1} and 1189 cm^{-1}[18].

The NMR spectra (supplementary data/Figs. S_5 – S_8) for the Schiff base ligands exhibit signals corresponding to the various chemical environments in the compounds. The characteristic azomethine proton (HC=N) for the sulphonamide Schiff bases resonated as a strong singlet at 8.47 - 8.31 ppm[34]. Similarly, the N-H signal for the imidazole and the sulfa moieties appeared downfield as a broad singlet at 6.71 ppm – 5.99 ppm in the spectra of the Schiff base ligands. In addition, the terminal NH_2 protons of L_1 resonated similarly as a broad signal at 7.26 ppm. The aromatic protons were observed as doublets at 7.76 – 7.68 ppm, while the strong singlet at 2.4 – 2.30 ppm corresponds to the methyl protons. The azomethine, C=N, was observed at 168.51 – 158.61 ppm instead. In addition, the signals at 141.36 – 90.29 ppm correspond to the aromatic C atoms, while the methyl carbon resonated at 23.89 – 12.36 ppm. The imidazole and the pyrimidine signals were observed at 158.29 – 153.50 ppm.

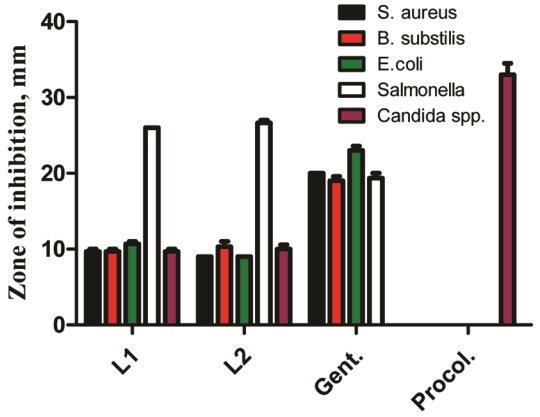

Fig. 1 — Antimicrobial activity of the sulphonamide-derived Schiff bases obtained from agar well diffusion assay showing moderate susceptibility of Salmonella spp. to L_1& L_2.

The electronic spectrum of ligand L_1(supplementary data/Fig. S_9) exhibited two distinct bands at 272 nm and 322 nm corresponding to the $\pi \rightarrow \pi^*$ and the $n \rightarrow \pi^*$ transitions of the azomethine, C=N, functional group[34]. The two transitions were, however, observed as a single broadband with wavelength maxima at 354 nm in the sulfamerazine-derived Schiff base (ligand L_2).

Antimicrobial study

The preliminary antimicrobial susceptibility study of the Schiff base compounds showed that *Salmonella spp*. was the most susceptible to all the tested organisms. The antibacterial inhibitory activity of both ligands L_1 and L_2 was higher than Gentamycin against *Salmonella spp*., as presented in Fig. 1. The two ligands, however, exhibited minimal inhibition

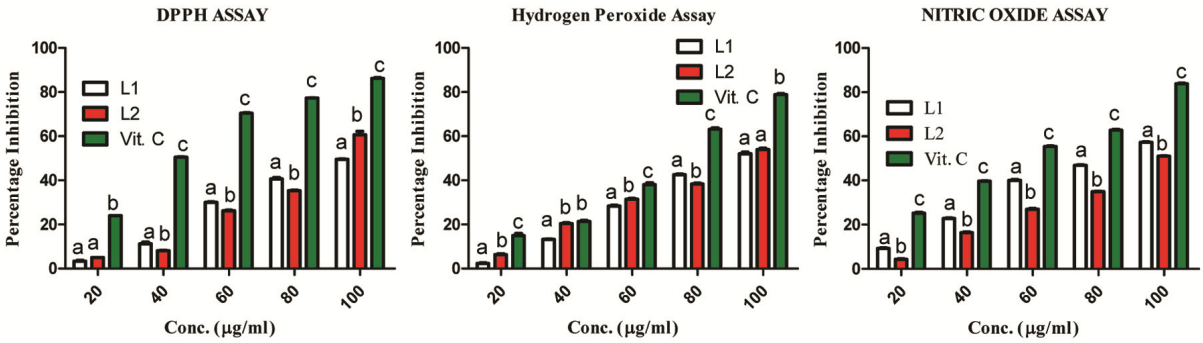

Fig. 2 — Radical scavenging activity of the sulphonamide Schiff bases, L_1 & L_2

Table 3 — [a]IC_{50} values for the radical scavenging activity (µg/mL)

Compound	DPPH	H_2O_2	NO
L_1	97.81	94.59	84.50
L_2	93.11	95.05	101.59
Vit. C	44.57	67.90	55.40

[a]IC_{50} is the half-maximal inhibitory concentration. The IC_{50} values were computed from the compounds' percentage inhibition of DPPH, H_2O_2, and NO free radicals using the Microsoft Excel package.

against *S. aureus, B. substilis, E. coli, and Candida spp*. In addition, *E. coli* was more susceptible than *B. substilis* and *Candida spp*. against ligand L_1, while both *E. coli* and *Candida spp*. were less susceptible to ligand L_2 than *B. substilis*.

The antibacterial activity of ligand L_2 against *Salmonella spp*. was slightly higher, with a MIC value of 0.625 µg/mL, compared with ligand L_1, having an MIC value of 1.25 µg/mL (supplementary data, Table 1). The bactericidal activity of the two sulphonamide-derived Schiff bases followed the trend observed for their minimum inhibitory concentrations with 1.25 and 2.5 µg/mL for ligands L_2 and L_1, respectively. This suggests that the sulfamerazine moiety induces higher antibacterial activity than the sulfaguanidine scaffold. Chohan *et al.* observed an increase in the activity of a series of salicylaldehyde-derived sulphonamide Schiff bases as the aliphatic chain on the sulphonamide moiety increases[35]. On the other hand, another study revealed that the antimicrobial activity of a series of sulphonamide Schiff bases varies with different microbial strains[18]. Furthermore, none of the compounds exhibited significant antifungal activity compared to procolazol, a standard antifungal agent.

Antioxidant Study

The radical scavenging activity of the sulphonamide-derived Schiff bases was evaluated using DPPH, hydrogen peroxide, and nitric oxide antioxidants assays at a concentration range of 20 – 100 µg/mL. The antioxidant activity of the compounds is expressed as percentage inhibition, as presented in Fig. 2, while the half-maximal inhibitory concentration (IC_{50}) values are presented in Table 3.

The sulfaguanidine Schiff base compound, ligand L_1, exhibited significant radical scavenging activity ($p < 0.005$) against nitric oxide free radicals than the sulfamethazine analog, L_2, across all the tested concentration range with IC_{50} values of 84.50 and 101.59 µg/ml for L_1 and L_2, respectively. Similarly, the radical scavenging ability of ligand L_1 against DPPH free radical was significantly higher than L_2 ($p < 0.001$) at 40 – 80 µg/mL. Ligand L_2, however, significantly ($p < 0.001$) exhibited better scavenging activity than L_1 at 100 µg/mL and 20 – 40 µg/mL concentrations against DPPH and hydrogen peroxide free radicals, respectively.

The free radical scavenging activity of the standard antioxidant drug, vitamin C, was much higher than the sulphonamide Schiff bases with IC_{50} values of 44.50 - 67.90 µg/ml against the DPPH, hydrogen peroxide, and nitric oxide free radicals. Lastly, L_1 and L_2 exhibited nearly the same scavenging ability against hydrogen peroxide radicals, with IC_{50} values of 94.59 and 95.05 µg/ml for L_1 and L_2, respectively.

Geometry optimization and electronic properties

The optimized geometries for the imidazole-derived sulphonamide ligands are presented in Fig. 3.

In addition, various electronic chemical reactivity descriptors for the molecules have been determined,

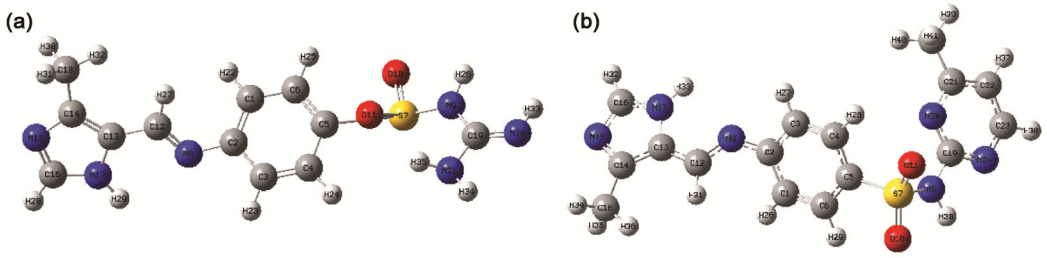

Fig. 3 — Optimized molecular structures for (a) L_1 (b) L_2 obtained from the DFT study. The structure is represented in a ball and stick model with carbon, nitrogen, sulphur, and oxygen atoms represented with grey, blue, yellow, and red balls respectively.

Table 4 — [a]Chemical Reactivity Descriptors for the Compounds

	LUMO (ev)	HOMO (ev)	ΔE (ev)	A (ev)	χ (ev)	μ (ev)	η (ev)	ω (ev)	S (ev)	I (ev)	α (a.u)	M Debye
L1	-2.06	-6.14	4.08	2.06	4.10	-4.10	2.04	4.12	0.49	6.14	260.90	1.71
L2	-2.20	-6.36	4.16	2.20	4.28	-4.28	2.08	4.40	0.48	6.36	294.07	5.77

as presented in Table 4, to rationalize the compounds' biological activity. The closeness of the values for the HOMO-LUMO energy gap (ΔE) for compounds L_1 (4.08 eV) and L_2 (4.16 eV) suggests similarity in the chemical reactivity of the two compounds. The values of the HOMO and LUMO energies are related to the electron affinity (A) and ionization energy (I) of the molecules according to Koopman's theorem, as illustrated in equations 2 and 3[36]. The sulphonamide compounds' electron affinity and ionization energies do not differ significantly.

$$A = -E_{LUMO} \quad ...2$$

$$I = -E_{HOMO} \quad ...3$$

Furthermore, the HOMO-LUMO energy gap is related to the global hardness (η) and softness (S) of the molecules, as shown in equations 4. Global softness is the reciprocal of global hardness. The global softness for L_1 and L_2 are 0.49 eV and 0.48 eV, respectively. Molecules with a higher energy gap (ΔE) exhibit higher global hardness and low softness. However, the global softness for L_1 and L_2 are nearly the same at 0.49 eV and 0.48 eV, respectively, indicating closer chemical reactivity.

$$\eta = \frac{\Delta E}{2} \quad ...4$$

Similarly, the electronic chemical potentials of the two compounds were approximated as negative values of the electronegativity values (χ) and obtained as – 4.10 eV and – 4.28 eV for L_1 and L_2, respectively. Molecules with higher chemical potential are less stable and exhibit higher reactivity. The higher reactivity of ligand L_2 was further substantiated by its high polarizability value of 294.07 a.u. compared to 260.90 a.u. for L1. Similarly, the dipole moment (μ) for L_2 is far greater than the value obtained for L_1, indicating higher chemical reactivity[37].

The frontier molecular orbital diagrams for the compounds (Fig. 4) revealed that the electron domain of the sulphonamide compounds is localized on the imidazole moiety and the sulphonyl scaffolds. However, the R group of the sulfa drug has a minimum contribution to the reactivity of the compounds. Consequently, the two imidazole-based sulphonamide ligands (L_1 and L_2) exhibited minimal differential reactivity.

Docking study

Molecular docking studies were conducted to assess the binding affinities and interactions of compounds L_1 and L_2 with six target proteins: cytochrome peroxidase (4AAO), myeloperoxidase (6WY7), NADPH oxidase (7U8G), xanthine oxidase (1N5X), dihydropteroate synthase (5V7A), and dihydrofolate reductase (4E4F). The details of the binding affinity values are presented in Table 5, while the representative ligand-protein complex interactions are presented in Figs. 5 and 6.

The docking results show that compound L_2 consistently exhibits superior binding affinities across all target proteins compared to L_1. Their inhibitory activity can be attributed to the observed favourable interaction profile, which includes a combination of hydrogen bonding, hydrophobic interactions, and van der Waals contacts within the protein binding sites.

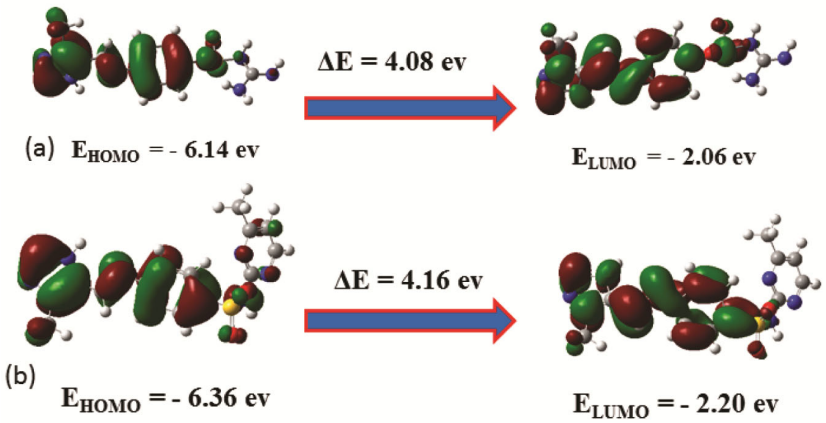

Fig. 4 — Frontier molecular orbitals for compounds (a) L_1 and (b) L_2, showing the electron domain and the HOMO-LUMO energy gap, ΔE.

Table 5 — Binding affinities and interactions of L_1 and L_2 against selected target proteins[a].

	4AAO	6WY7	7U8G	1N5X	4E4F	5V7A
L_1						
Binding Affinity (kcal/mol)	-7.5	-9.5	-9	-8.6	-7.2	-7.6
Hydrogen bond interaction	3	2	6	6	5	2
Hydrophobic interaction	9	4	6	3	6	2
Electrostatic interaction	3	5	0	1	0	1
Van der Waals interaction	8	9	8	8	9	8
Unfavourable (repulsion)	0	1	1	3	1	1
L_2						
Binding Affinity (kcal/mol)	-8.7	-9.7	-9.7	-9.6	-8.3	-8.9
Hydrogen bond interaction	3	2	4	7	2	5
Hydrophobic interaction	5	5	5	4	10	1
Electrostatic interaction	1	2	1	1	0	2
Van der Waals interaction	7	10	11	7	10	9
Unfavourable (repulsion)	0	0	0	0	0	0

[a]Binding affinities are obtained from docking results using AutoDock vina[24,] and binding interactions are visualized with BIOVIA discovery studio. Cytochrome peroxidase (4AAO), myeloperoxidase (6WY7), NADPH oxidase (7U8G), xanthine oxidase (1N5X), dihydropteroate synthase (5V7A), and dihydrofolate reductase (4E4F).

The binding affinities (in kcal/mol) for L_2 are more negative across all targets, with values of –8.3 to –9.7 kcal/mol, as opposed to L_1's range of –7.2 to –9.5 kcal/mol. This trend suggests a more stable binding conformation for L_2, implying that it may act as a potent inhibitor of these targets[36].

L_1 and L_2 show reasonable hydrogen bond interactions across all complexes within the docking studies. These interactions are crucial for the specificity and stability of ligand binding within protein targets, as hydrogen bonds provide both directional and stabilizing effects that anchor the ligand in the active site, reducing the possibility of dissociation and improving overall binding strength[38]. Hydrophobic interactions further support the observed binding performance of both L_1 and L_2. Hydrophobic interactions are particularly advantageous in non-polar binding environments, where they drive the ligand deeper into the protein's hydrophobic core, thereby contributing to binding stability and affinity[39].

ADMET properties and drug-likeness

The drug-likeness and pharmacokinetic properties of L_1 and L_2 were evaluated using ADMETlab3.0, and the results are summarized in Table 6. Lipinski's rule of five, a benchmark for assessing oral bioavailability, sets the following thresholds for drug-likeness: molecular weight (MW) ≤ 500 Da, LogP ≤ 5, hydrogen bond donors ≤ 5, and hydrogen bond acceptors ≤ 10. L_1 and L_2 meet these criteria, indicating potential for effective oral bioavailability[33].

Absorption potential was evaluated through Caco-2 and Madin-Darby Canine Kidney (MDCK) permeability indices. While the Caco-2 permeability threshold of −5.15 often indicates high intestinal permeability, only L_2 approaches this range, whereas

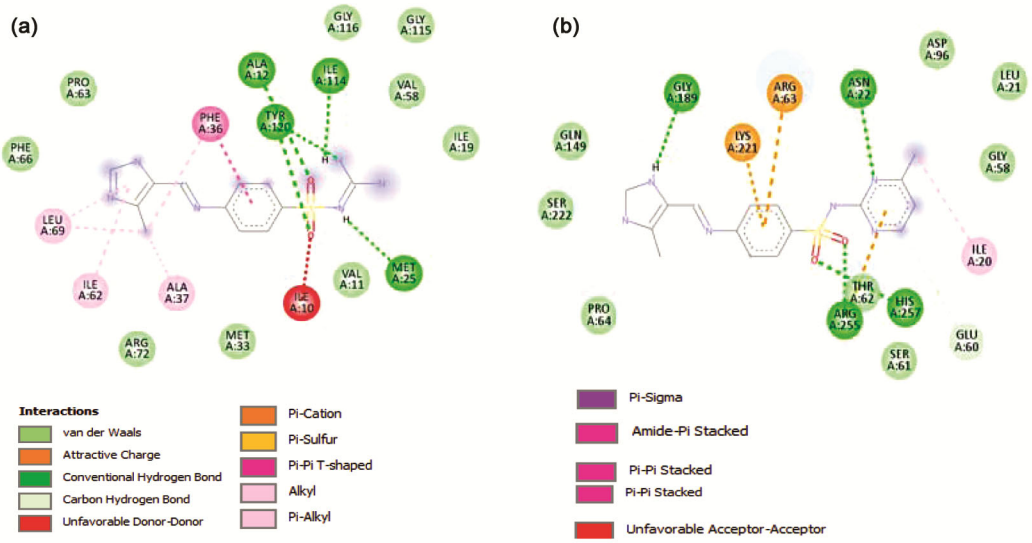

Fig. 5 — Binding interactions of the compounds with DHPS (PDB ID: 5V7A protein. (a) L_1 - DHPS (PDB ID: 5V7A) complex (b) L_2 - DHPS (PDB ID: 5V7A). Amino acid residues of the protein are represented as discs, while ligand L_2 is depicted as lines. Intermolecular interactions are coloured according to the type of interactions.

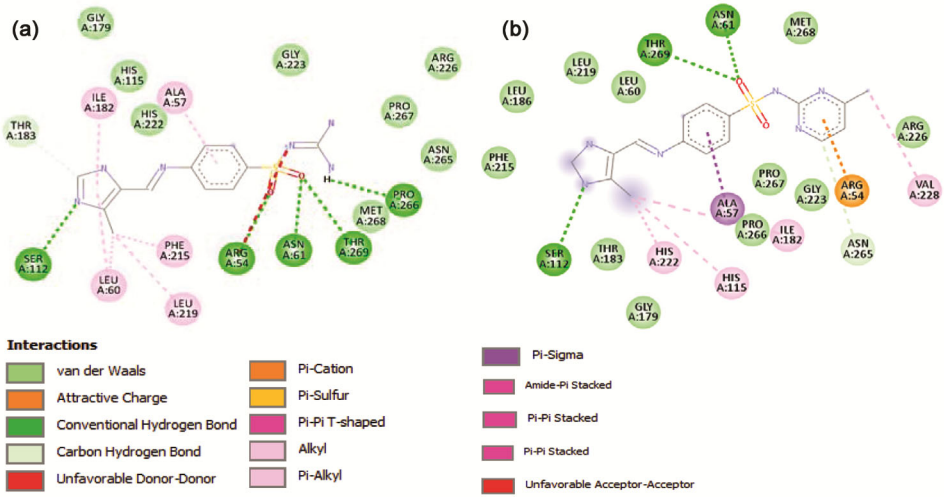

Fig. 6 — Binding interactions of the compounds with NADPH oxidase (PDB ID: 7U8G). (a) L_1 - NADPH oxidase complex (b) L_2 - NADPH oxidase complex. Amino acid residues of the protein are represented as discs, while ligand L_2 is depicted as lines. Intermolecular interactions are coloured according to the type of interactions.

L_1 does not fully meet this criterion. Nonetheless, L_1 and L_2 surpass the MDCK threshold of 2×10^{-6} cm/s, suggesting high overall permeability and potential for blood-brain barrier (BBB) penetration[40]. Both compounds' interactions with P-glycoprotein (Pgp), a key transporter associated with drug efflux, were also investigated. The results demonstrated that L_1 and L_2 function effectively as Pgp inhibitors and substrates, with binding values within the recommended range of 0–0.3, further supporting their favorable pharmacokinetic profiles. Additionally, human oral bioavailability indices, $F_{20\%}$, and $F_{30\%}$ fall within the acceptable 0–0.3 range underscoring the compounds' viability for oral administration. The human intestinal absorption (HIA) index also returned values within the standard range, confirming high absorptive capacity[32].

To assess cardiotoxicity, a critical factor for drug safety, hERG (human ether-a-go-go-related gene) inhibition was measured, as hERG channels play an essential role in cardiac function. L_1 and L_2 exhibited hERG inhibition within the safe 0-0.3 range, implying low cardiotoxic risk[32]. Additional toxicity screenings, including assessments for Ames's mutagenicity, rat oral

Table 6 — ADMET parameters and drug-likeness properties of L_1 and L_2[a].

	Observed Values			Observed values	
Parameters	L_1	L_2	Parameters	L_1	L_2
HBD	5	3	$F_{20\%}$	0.003	0.015
HBA	8	8	$F_{30\%}$	0.004	0.182
MW (g/mol)	306.09	358.12	Golden triangle	Pass	Pass
PSA	137.08	108.37	Lipinski rule	Pass	Pass
Rotatable bonds	5	5	Pfizer rule	Pass	Pass
LogP	-0.229	0.774	GSK rule	Pass	Pass
QED	0.486	0.702	Rat oral acute	0.418	0.012
VDss (human)	0.336	-0.195	FDAMDD	0.261	0.003
Pgp-substrate	0.328	0.055	AMES	0.224	0.036
Pgp-inhibitor	0	0.001	Respiratory	0.333	0.002
Caco2 permeability	-6.18	-5.29	hERG blockers	0.067	0.023
MDCK permeability	0.1	0	IGC_{50}	2.762	2.903
HIA	0.001	0	$LC_{50}FM$	3.4	3.547
BBB penetration	0.011	0.212	$LC_{50}DM$	4.439	4.27

[a]ADMET parameters and drug-likeness properties are obtained from ADMETlab3.0 web server[32].

toxicity, skin sensitization, FDA maximum daily dose (FDAMDD), and respiratory toxicity, yielded results within permissible safety limits for both compounds, further confirming a low toxicity profile[41].

Conclusion

Sulphonamide Schiff base compounds, L_1 and L_2, containing the imidazole nucleus, have been synthesized. Both compounds exhibited moderate antimicrobial activity against *Salmonella spp*. Ligand L_1 was a better scavenger for nitric oxide free radicals at all tested concentrations (20 – 80 µg/mL). L_2 exhibited a slightly higher radical scavenging activity against DPPH radicals at high concentrations (100 µg/mL). The DFT and the docking study of the optimized geometries of the compounds substantiated the inhibitory effects of the two compounds. Lastly, the quantitative estimate of drug-likeness (QED) for L_1 and L_2 suggests that they are promising candidates for further drug development.

Acknowledgements

We are grateful to Lagos State University, Ojo, for partially funding this project through the TETFund IBR research grant. We also acknowledge the effort of Dr. Joseph Adekoya, Covenant University, Ota, for the UV-Vis analysis of the compounds. Lastly, we appreciate Mr. Olayinka Onifade of Lagos University Teaching Hospital (LUTH), Idi-Araba, for the antioxidant bioassay.

Supplementary Information

Supplementary information is available in the website http://nopr.niscpr.res.in/handle/123456789/58776.

References

1 Then R, *Dihydropteroate Synthase* in *Pharm Comp Pharmacol Ref*, *Enna S J, Bylund D B,* Ed., (Elsevier, Amsterdam) 2007.
2 Plumlee K H, *Pharmaceuticals* in *Clin Vet Toxicol*, Ed., (Elsevier, Amsterdam) 2004.
3 Genç Y, Özkanca R&Bekdemir Y, *Ann Clin Microbiol Antimicrob,* **7** (2008) 1.
4 Dash R N, Moharana A K & Subudhi B B, *Curr Org Chem,* 24 (2020) 1018.
5 Thach T-D, Nguyen T M-T, Nguyen T A-T, Dang C-H, Luong T-B, Dang V-S, Banh K-S, LucV-S & Nguyen T-D, *Arab J Chem,* 14 (2021) 103408.
6 Wan Y, Fang G, Chen H, Deng X & Tang Z, *Eur J Med Chem,* 226 (2021) 113837.
7 Akocak S, Mehmet B, Lolak N, Tuneg M & Sanku R K K, *J Turkish Chem Soc Sect A Chem,* 6 (2019) 63.
8 Hida S, Yoshida M, Nakabayashi I, Miura N N, Adachi Y & Ohno N, *Biol Pharm Bull,* 28 (2005) 773.
9 Ghosh A K, Kincaid J F, Cho W, Walters D E, Krishnan K, Hussain K A, Koo Y, Cho H, Rudall C & Holland L, *Bioorg Med Chem Lett,* 8 (1998) 687.
10 Masini E, Carta F, Scozzafava A & Supuran C T, *Expert Opin Ther Pat,* 23 (2013) 705.
11 Laragh J H & Sealey J E, *Hypertension,* 37 (2001) 806.
12 Li J J, Anderson G D, Burton E G, Cogburn J N, Collins J T, Garland D J, Gregory S A, Huang H –C & Isakson P C, *J Med Chem,* 38 (1995) 4570.
13 Kumar H, Manoharan A, Anbarasu A & Ramaiah S, *Gene,* 851 (2023) 146995.
14 Sköld O, *Vet Res,* 32 (2001) 261.
15 Chen M, Chen X, Huang G, Jiang Y, Gou Y & Deng J, *J Mol Struct,* 1268 (2022) 133730.
16 Sandhu Q -U -A, Pervaiz M, Majid A, Younas U, Saeed Z, Ashraf A, Khan R R M, Ullah S, Ali F & Jelani S, *J Coord Chem*, (2023) 1.
17 Garoufis A, Hadjikakou S K & Hadjiliadis N, *Coord Chem Rev,* 253 (2009) 1384.
18 Mondal S, Mandal S M, Mondal T K & Sinha C, *J Mol Struct,* 1127 (2017) 557.
19 Magaldi S, Mata-Essayag S, De Capriles C H, Pérez C, Colella M T, Olaizola C & Ontiveros Y, *Int J Infect Dis,* 8 (2004) 39.

20 Wiegand I, Hilpert K & Hancock R E W, *Nat Prot,* 3 (2008) 163.
21 Kedare S B & Singh R P, *J Food Sci Technol,* 48 (2011) 412.
22 Ali B M, Boothapandi M & Nasar A S, *Data Br,* 28 (2020) 104972.
23 Ruch R J, Cheng S & Klaunig J E, *Carcinogenesis,* 10 (1989) 1003.
24 Eberhardt J, Santos-Martins D, Tillack A F & Forli S, *J Chem Inf Model,* 61 (2021) 3891.
25 Seidel J, Hoffmann M, Ellis K E, Seidel A, Spatzal T, Gerhardt S, Elliott S J & Einsle O, *Biochem*, 51 (2012) 2747.
26 Strzelczyk P, Zhang D, Dyba M, Wlodawer A & Lubkowski J, *Sci Rep,* 10 (2020) 17516.
27 Noreng S, Ota N, Sun Y, Ho H, Johnson M, Arthur C P, Schneider K, Lehoux I, Davies C W & Mortara K, *Nat Comm,* 13 (2022) 6079.
28 Okamoto K, Eger B T, Nishino T, Kondo S, Pai E F & Nishino T, *J Biol Chem*, 278 (2003) 1848.
29 Dennis M L, Lee M D, Harjani J R, Ahmed M, DeBono A J, Pitcher N P, Wang Z, Chhabra S, Barlow N & Rahmani R, *Chem Eur J*, 24 (2018) 1922.
30 Lange K, Frey K M, Eck T, Janson C A, Gubler U & Goodey N M, *PLoS Negl Trop Dis*, 17 (2023) e0011303.
31 KochnevY & Durrant J D, *J Cheminfo*, 14 (2022) 58.
32 Fu L, Shi S, Yi J, Wang N, He Y, Wu Z, Peng J, Deng Y, Wang W & Wu C, *Nucleic Acids Res,* (2024) gkae236.
33 Lipinski C A, *Drug Discov Today Tech,* 1 (2004) 337.
34 Sobola A O & Watkins G M, *J Serbian Chem Soc,* 83 (2018) 809.
35 Chohan Z H, Mahmood-Ul-Hassan, Khan K M & Supuran C T, *J Enzyme Inhib Med Chem,* 20 (2005) 183.
36 Rana K M, Maowa J, Alam A, Dey S, Hosen A, Hasan I, Fujii Y, Ozeki Y & Kawsar S M A, *Silico Pharm,* 9 (2021) 1.
37 Bulbul M Z H, Hosen M A, Ferdous J, Chowdhury T S, Misbah M M H & Kawsar S, *Int J New Chem,* 8 (2021) 88.
38 Nittinger E, Inhester T, Bietz S, Meyder A, Schomburg K T, Lange G, Klein R & Rarey M, *J Med Chem,* 60 (2017) 4245.
39 Liu K, Zha X-Q, Li Q-M, Pan L-H & Luo J-P, *Food Hydrocoll*, 118 (2021) 106807.
40 Geldenhuys W J, Mohammad A S, Adkins C E & Lockman P R, *Ther Deliv*, 6 (2015) 961.
41 Sulistyowaty M I, Widyowati R, Putra G S, Budiati T & Matsunami K, *J Bas Clin Phys Pharm*, 32 (2021) 385.